AMERICAN SOCIETY FOR MICROBIOLOGY | Journal of Virology®

PATHOGENESIS AND IMMUNITY

Chemokine Receptor Ccr7 Restricts Fatal West Nile Virus Encephalitis

Susana V. Bardina,[a,b] Julia A. Brown,[a,b] Daniela Michlmayr,[b]* Kevin W. Hoffman,[a,b] Janet Sum,[b]* Alexander G. Pletnev,[c] Sergio A. Lira,[d] Jean K. Lim[b]

The Graduate School of Biomedical Sciences, Icahn School of Medicine at Mount Sinai, New York, New York, USA[a]; Department of Microbiology, Icahn School of Medicine at Mount Sinai, New York, New York, USA[b]; Laboratory of Infectious Diseases, National Institute of Allergy and Infectious Diseases, National Institutes of Health, Bethesda, Maryland, USA[c]; Immunology Institute, Icahn School of Medicine at Mount Sinai, New York, New York, USA[d]

ABSTRACT West Nile virus (WNV) is a mosquito-transmitted flavivirus that can cause debilitating encephalitis. To delineate the mechanisms behind this pathology, we studied Ccr7-deficient mice, which afforded us the capacity to study infection in mice with disrupted peripheral cellular trafficking events. The loss of Ccr7 resulted in an immediate pan-leukocytosis that remained elevated throughout the infection. This leukocytosis resulted in a significant enhancement of leukocyte accumulation within the central nervous system (CNS). Despite an excess of virus-specific T cells in the CNS, Ccr7-deficient mice had significantly higher CNS viral loads and mortality rates than wild-type animals. Mechanistically, the elevated trafficking of infected myeloid cells into the brain in Ccr7-deficient mice resulted in increased levels of WNV in the CNS, thereby effectively contributing to neuroinflammation and lowering viral clearance. Combined, our experiments suggest that during WNV infection, Ccr7 is a gatekeeper for nonspecific viral transference to the brain.

IMPORTANCE In this study, we show that Ccr7 is required for the sufficient migration of dendritic cells and T cells into the draining lymph node immediately following infection and for the restriction of leukocyte migration into the brain. Further, the severe loss of dendritic cells in the draining lymph node had no impact on viral replication in this organ, suggesting that WNV may migrate from the skin into the lymph node through another mechanism. Most importantly, we found that the loss of Ccr7 results in a significant leukocytosis, leading to hypercellularity within the CNS, where monocytes/macrophages contribute to CNS viremia, neuroinflammation, and increased mortality. Together, our data point to Ccr7 as a critical host defense restriction factor limiting neuroinflammation during acute viral infection.

KEYWORDS arbovirus, cell trafficking, chemokine receptors, chemokines, host-pathogen interactions, leukocytes, neuroimmunology, viral pathogenesis

West Nile virus (WNV) is a mosquito-transmitted flavivirus that was introduced into the United States in 1999 (1). Since then, the virus has spread rapidly across the continent and has become the leading cause of arthropod-borne virus-induced encephalitis in the United States. WNV is a significant public health concern due to the unpredictable nature of annual disease outbreaks and the lack of specific therapeutics and vaccines for human use (2). In humans, WNV is transmitted through the bite of an infected mosquito. The outcome of infection ranges from asymptomatic to severe neuroinvasive disease, including meningitis, encephalitis, and/or acute flaccid paralysis (3–5). Through 2016, WNV has caused 21,035 cases of neurological disease, with approximately 9% mortality (Centers for Disease Control and Prevention [www.cdc.gov]).

Received 13 December 2016 **Accepted** 7 March 2017

Accepted manuscript posted online 29 March 2017

Citation Bardina SV, Brown JA, Michlmayr D, Hoffman KW, Sum J, Pletnev AG, Lira SA, Lim JK. 2017. Chemokine receptor Ccr7 restricts fatal West Nile virus encephalitis. J Virol 91:e02409-16. https://doi.org/10.1128/JVI.02409-16.

Editor Jae U. Jung, University of Southern California

Address correspondence to Jean K. Lim, jean.lim@mssm.edu.

* Present address: Daniela Michlmayr, Division of Infectious Diseases and Vaccinology, School of Public Health, University of California, Berkeley, Berkeley, California, USA; Janet Sum, Department of Medicine, Columbia University Medical Center, New York, New York, USA.

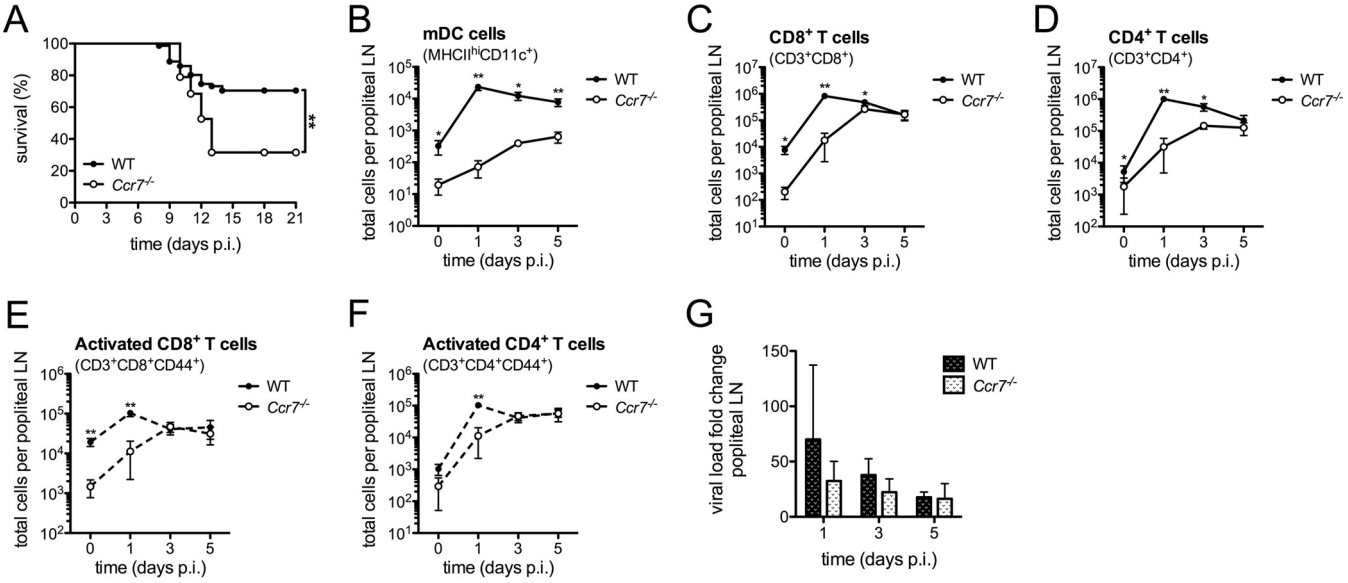

FIG 1 Ccr7 is required for survival and directs DCs and T cells to the draining lymph node during WNV infection. (A) Kaplan-Meier survival analysis of WNV-infected WT ($n = 69$) and *Ccr7*$^{-/-}$ ($n = 36$) mice. Data shown are pooled from three independent experiments. (B to F) Following forward scatter/side scatter and UV-negative gating for live cells, total cell numbers of mDCs (MHC-II^{hi} CD11c^{+}), CD8^{+} T cells (CD3^{+} CD8^{+}), CD4^{+} T cells (CD3^{+} CD4^{+}), activated CD8^{+} T cells (CD3^{+} CD8^{+} CD44^{+}), and activated CD4^{+} T cells (CD3^{+} CD4^{+} CD44^{+}) were assessed by flow cytometry from the popliteal lymph node (LN) from WT and *Ccr7*$^{-/-}$ mice. (G) Virus load was quantified in the popliteal LN by quantitative RT-PCR. All data are shown as means ± standard deviations for $n =$ 3 to 8 mice per genotype and time point from two independent experiments. *, $P < 0.05$; **, $P < 0.01$. p.i., postinfection; LN, lymph node.

Following peripheral inoculation in mice, initial WNV replication is thought to occur in skin Langerhans cells that then traffic to the draining lymph node, where further replication occurs (6–8). Viremia ensues, followed by infection of secondary lymphoid and visceral organs (9). In some cases, the virus enters the central nervous system (CNS), where neurons are the primary target (10). The infiltration of effector antiviral T cells is critical for successful viral control in the CNS, which requires proper initiation and activation events in the periphery (11–14). The importance of dendritic cell-T cell interactions immediately following infection in the periphery and the impact of this interaction on the development of the antiviral response to WNV infection are currently unknown.

Chemokine receptor Ccr7 is expressed by numerous cell types, including dendritic cells (DC), T cells, and neutrophils (15, 16). During homeostasis, Ccr7 regulates the homing of T cells into lymphoid organs, such as the lymph nodes. Furthermore, DCs upregulate Ccr7 following activation, which allows their efficient entry into terminal lymphatics expressing its cognate ligand Ccl21. These processes promote efficient DC-T cell interactions to enable priming of T cells, leading to their differentiation into effector T cells (16, 17). Ccr7 is also expressed on CNS-resident cells, including microglia and astrocytes, although the role of these cell types during peripheral infection with a neurotropic virus has been understudied (18, 19). In the manuscript, we evaluate the impact of Ccr7 in regulating WNV pathogenesis in a mouse model of infection.

RESULTS

Ccr7 is required for survival as well as DC and T cell trafficking to lymph nodes following WNV infection. To evaluate the importance of Ccr7 in the host response to WNV, wild-type (WT) and *Ccr7*$^{-/-}$ mice were infected with WNV through footpad injection. We observed a significant increase in mortality in the Ccr7-deficient mice compared to that in WT mice during WNV infection ($P = 0.0004$) (Fig. 1A). Thus, Ccr7 is a critical host response protein required for survival following WNV infection *in vivo*. Given the role of Ccr7 in the migration of dendritic cells from the skin into the draining lymph node following activation (6, 20), we next evaluated the impact of this receptor on this migration event and its subsequent effect on T cell activation. Under homeo-

static conditions, Ccr7-deficient mice showed a drastic decrease in the number of myeloid dendritic cells (mDCs) positive for CD11c and expressing high levels of major histocompatibility complex class II ($CD11c^+$ MHC-II^{hi}) in comparison to the numbers in WT mice, as expected (WT mice, $n = 333$; *Ccr7*$^{-/-}$ mice, $n = 24$ [mean cell number]) (Fig. 1B). At the peak of mDC infiltration into the lymph node, where an ~72-fold increase was observed compared to the level under uninfected conditions, only an ~4-fold increase in mDC accumulation was observed in the Ccr7-deficient mice. Given that T cells utilize Ccr7 to home to the draining lymph nodes during homeostasis and inflammation (16, 17), the total number of $CD8^+$ and $CD4^+$ T cells within the popliteal lymph node following infection was counted and found to be decreased at day 0 (mean number of $CD8^+$ T cells in WT mice, $n = 18{,}362$, and in *Ccr7*$^{-/-}$ mice, $n = 3{,}575$; mean number of $CD4^+$ T cells in WT mice, $n = 17{,}670$ and in *Ccr7*$^{-/-}$ mice $n = 8{,}804$) and days 1 and 3 postinfection in Ccr7-deficient mice (Fig. 1C and D). This defect was transient since $CD8^+$ or $CD4^+$ T cell numbers eventually reached levels comparable to those of WT mice by day 5. Since the interaction of DCs and T cells is critical for effective T cell activation following infection, we also evaluated the kinetics of T cell activation by monitoring CD44 expression (Fig. 1E and F). For both $CD8^+$ and $CD4^+$ T cells, there was an increase in the total number of $CD44^+$ activated T cells following infection in the draining lymph node, with a transient delay observed in *Ccr7*$^{-/-}$ mice that essentially disappeared by day 3. Thus, our data show that Ccr7 is required for efficient mDC and T cell migration into the lymph node during early infection, and the absence of Ccr7 transiently delays T cell activation.

For mosquito-transmitted flaviviruses such as WNV, it is believed that dendritic cells infected within the skin carry the virus from the site of infection into the draining lymph node (6, 20). Given that the accumulation of mDCs into the draining lymph node is greatly impaired in the absence of Ccr7, we evaluated the subsequent impact on viral replication in the draining lymph node by quantifying viral genome equivalents following infection. As shown in Fig. 1G, virus was detected in both WT and *Ccr7*$^{-/-}$ mice to similar degrees on days 1, 3, and 5 postinfection. No virus was detected in the blood after day 5. Surprisingly, viral measurements taken in the draining lymph node did not differ in the presence or absence of Ccr7, despite the significant loss of mDCs, suggesting that the virus may traffic to the draining lymph node through another mechanism.

Leukocytes and proinflammatory cytokines are elevated in the blood of WNV-infected *Ccr7*$^{-/-}$ mice. Given the defect in mDC and T cell migration in the draining lymph node in the absence of Ccr7, we evaluated whether the peripheral response to WNV would also be altered. To test this, we assessed the total number of leukocyte subsets in circulation following WNV infection. Unexpectedly, we observed significantly elevated numbers of circulating $CD8^+$ T cells, $CD4^+$ T cells, monocytes, and neutrophils during infection (Fig. 2A to D). This was not observed for all cell types as NK and B cells remained unaltered (Fig. 2E and F). Analysis of $CD8^+$ and $CD4^+$ T cell activation via CD44 expression revealed an excess number of activated T cells in the blood of WT mice in comparison to that in Ccr7-deficient mice during infection (Fig. 2G and H). Examination of cytokine/chemokine levels in the plasma revealed increased levels of chemokines Ccl2 and Ccl7 involved in monocytosis and neutrophilia (21, 22), as well as of T cell chemoattractants Ccl4 and Cxcl9 (Fig. 2I to L), a profile consistent with an enhanced proinflammatory state. Concomitantly, a significant decrease in the anti-inflammatory cytokine interleukin-10 (IL-10) was also found (Fig. 2M). Despite these differences, we found no difference in the abilities of these mice to clear virus in the periphery, with viral measurements in the peripheral blood nearly identical at all time points tested (Fig. 2N). Together these data suggest that Ccr7 may provide a retention signal for myeloid and T cells in the draining lymph node, the loss of which causes a dysregulation of leukocytes in the periphery.

Loss of Ccr7 does not impact leukocyte accumulation or T cell priming in the spleen during WNV infection. We next evaluated whether Ccr7 contributes to leukocyte accumulation in other peripheral organs, such as the spleen. Evaluation of the

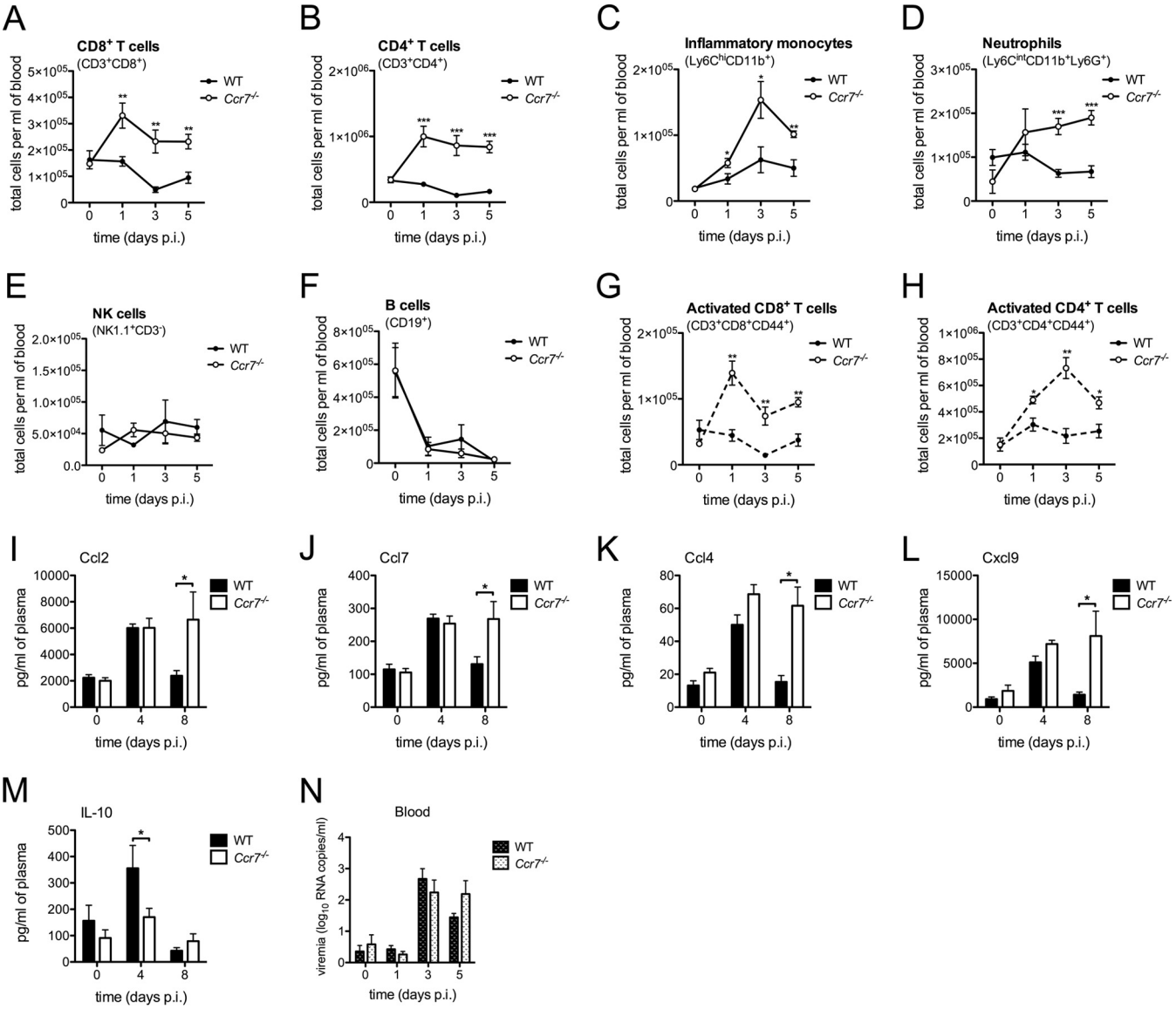

FIG 2 Leukocytes and proinflammatory cytokines are elevated in the blood of WNV-infected *Ccr7*$^{-/-}$ mice. (A to H) Following forward scatter/side scatter and UV-negative gating for live cells, total cell numbers of CD8$^+$ T cells (CD3$^+$ CD8$^+$), CD4$^+$ T cells (CD3$^+$ CD4$^+$), monocytes (Ly6C^{hi} CD11b$^+$), neutrophils (Ly6C^{int} CD11b$^+$ Ly6G$^+$), NK cells (NK1.1$^+$ CD3$^-$), B cells (CD19$^+$), activated CD8$^+$ T cells (CD3$^+$ CD8$^+$ CD44$^+$), and activated CD4$^+$ T cells (CD3$^+$ CD4$^+$ CD44$^+$) were assessed by flow cytometry on days 0, 1, 3, and 5 postinfection from the blood of WT and *Ccr7*$^{-/-}$ mice. (I to M) Protein levels of cytokines and chemokines Ccl2, Ccl7, Ccl4, Cxcl9, and IL-10 in the blood of WT and *Ccr7*$^{-/-}$ mice at day 0 and at 4 and 8 days postinfection were measured by multiplex ELISA. (N) Virus load was quantified in the blood plasma by quantitative RT-PCR. All data are shown as means ± standard deviations for $n = 4$ mice per genotype and time point from three independent experiments. *, $P < 0.05$; **, $P < 0.01$; ***, $P < 0.001$.

number of CD8$^+$ T cells, CD4$^+$ T cells, inflammatory monocytes, neutrophils, activated CD8$^+$ T cells, activated CD4$^+$ T cells, and viral loads in the spleen of WT and Ccr7-deficient mice following WNV infection revealed no changes (see Fig. S1A to G in the supplemental material). Given the delay in early DC-T cell accumulation in the lymph node and the excessive numbers of T cells in circulation, we next evaluated whether the development of T cell subsets, Th17 cells and regulatory T (Treg) cells, known to be important during WNV infection was altered (23–28). Peripheral IL-17 production from CD4$^+$ T cells and the numbers of CD4$^+$ FoxP3$^+$ Treg cells from splenocytes of WT and *Ccr7*$^{-/-}$ mice at day 8 were measured, but no change in the percentage of either cell type was observed (Fig. S1H and K). Further evaluation of WNV-specific effector activity of CD8$^+$ T cells through *ex vivo* production of gamma interferon (IFN-γ) and tumor necrosis factor alpha (TNF-α) following stimulation with the immunodominant T cell

epitope NS4B WNV-specific peptide (14, 29) showed no differences in percentages and numbers of cells between WT and *Ccr7*$^{-/-}$ mice (Fig. S1I, J, and L). Taking these observations together, it appears that although the absence of Ccr7 results in dysregulation of circulating T cell numbers, there appears to be no defect in T cell activation or functionality during WNV infection.

Leukocyte infiltration into the CNS is enhanced in WNV-infected *Ccr7*$^{-/-}$ mice. We next evaluated whether the hypercellularity observed in the blood of *Ccr7*$^{-/-}$ mice would impact the migration of leukocytes into the CNS. By day 8, the total numbers of CD8$^+$ and CD4$^+$ T cells in the brain were significantly elevated in WNV-infected *Ccr7*$^{-/-}$ mice in comparison to levels in WT mice, and this was even more pronounced by day 12, while the percentages of these cell populations remained unchanged (Fig. 3A to C). This observation held true for inflammatory monocytes and neutrophils at day 12 (Fig. 3E to G). There was no difference in NK cell numbers during all time points tested (data not shown). To evaluate this in greater detail, we conducted immunohistochemistry on WT and *Ccr7*$^{-/-}$ mouse brain tissue on day 12 by staining for MAC2 (myeloid marker), myeloperoxidase (neutrophil marker), and CD3 (T cell marker) (Fig. 3D). Within the perivascular, parenchymal, and meningeal regions of the CNS, enhanced staining for monocytes, neutrophils, and T cells (indicated by black arrows) was observed in *Ccr7*$^{-/-}$ mice (Fig. 3D shows representative images). This trend is concurrent with the enhanced total number of these cell types found in the CNS of *Ccr7*$^{-/-}$ mice by flow cytometry. Regardless, the WT and Ccr7-deficient T cells were activated to the same extent, as demonstrated by their expression of the CD44 activation marker (Fig. 3H and I), and their ability to produce IFN-γ remained unchanged between strains (data not shown). Of note, the production of Ccr7 ligands, Ccl19 and Ccl21, was not altered in the brain in either strain (Fig. 3J and K). As lack of recruitment of mDCs to the CNS leads to higher numbers of infiltrating T cells and inefficient viral control (30), mDC numbers in the CNS were calculated at day 8 postinfection, and we found no change in the numbers of mDCs in the CNS between WT and Ccr7-deficient mice (Fig. 3L). Furthermore, Treg cell numbers in the CNS were evaluated as decreased Treg cell numbers in the brains of mice at day 8 postinfection were associated with enhanced viral titers in the brain and mortality (28), and we found no change in Treg cell numbers in the CNS between WT and Ccr7-deficient mice (Fig. 3M). Thus, it appears that the hypercellularity induced by the loss of Ccr7 may impact inflammation within the CNS by promoting leukocyte infiltration.

Ccr7-deficient mice have a defect in CNS viral clearance. We next evaluated whether the increased infiltration of antiviral T cells into the CNS impacted viral clearance in the brain. To do this, we measured viral loads within the CNS of WT and Ccr7-deficient mice on days 8 and 12 by a focus forming unit (FFU) assay. As shown in Fig. 4A, similar levels of virus were observed in WT and *Ccr7*$^{-/-}$ mice on day 8. However, by day 12, viral loads decreased in WT mice, while viral levels in *Ccr7*$^{-/-}$ mice remained elevated ($P = 0.004$). Immunofluorescence analysis confirmed elevated viral loads in *Ccr7*$^{-/-}$ mice throughout the CNS, particularly in the cerebellum and hippocampus (Fig. 4B). Together, these data show that Ccr7 is needed for survival of WNV infection and proper viral control in the CNS.

Ccr7 deficiency leads to increased neuroinflammation in WNV-infected mice. As the total numbers of CD8$^+$ T cells are elevated in the CNS, we assessed whether this increase would contribute to the hyperinflammatory state in the CNS. To test this, we measured the total protein levels of IFN-γ and TNF-α on days 8 and 12 in the CNS. As shown in Fig. 5A and B, IFN-γ levels were significantly elevated on day 10, and TNF-α levels were elevated on days 8 and 10. Given that CD4$^+$ T cell, monocyte, and neutrophil numbers are also elevated within the CNS, we evaluated cytokines within the CNS associated with these cell types. A reproducible and significant decrease in IL-1β was observed on day 8 in the absence of Ccr7 compared to the level in WT mice (Fig. S2A). This was followed by a significant increase in numerous proinflammatory cytokines (IL-12 and IL-22) and cytokine/chemokines (Ccl3 to Ccl5, Ccl2, and Ccl7) on

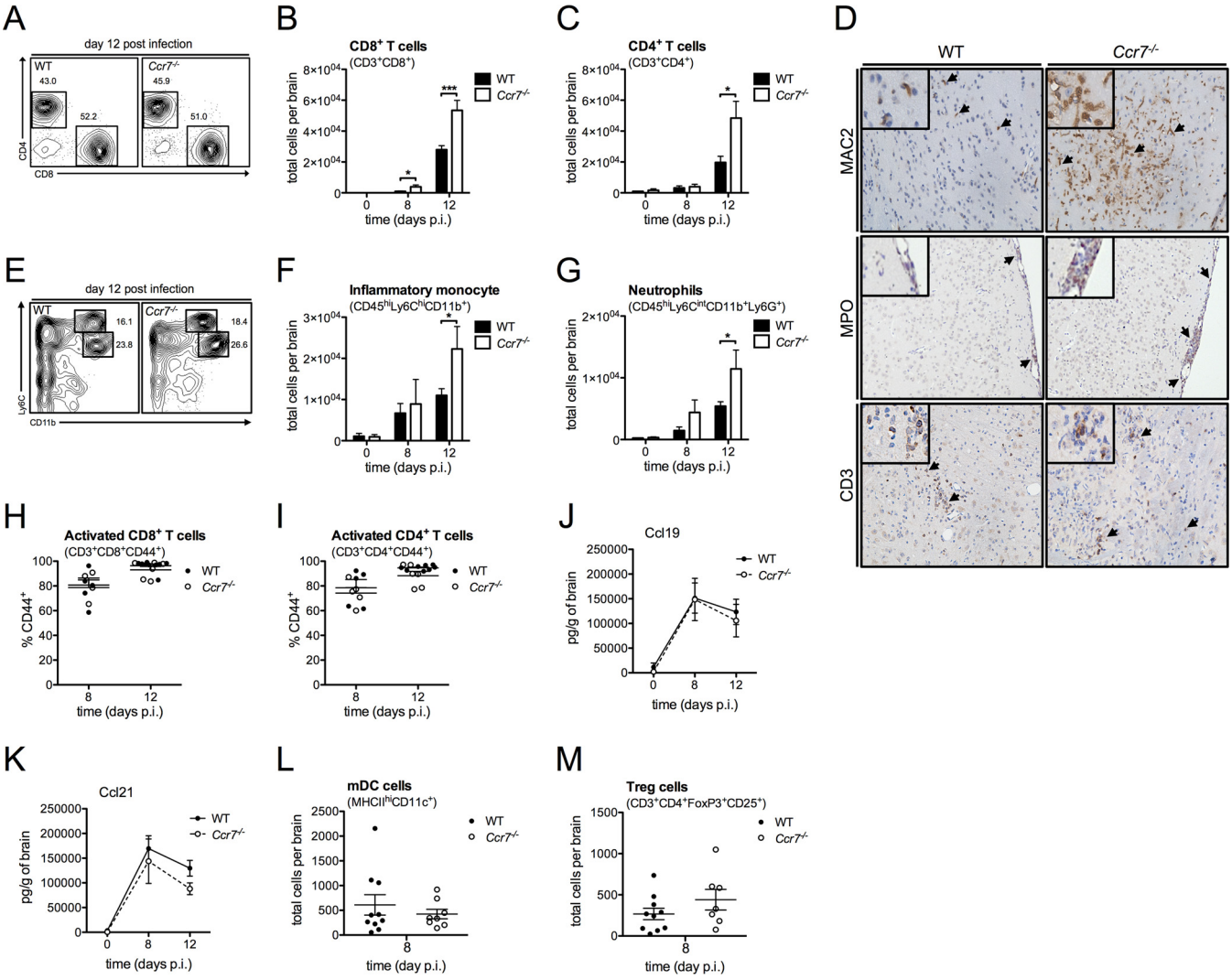

FIG 3 Leukocyte infiltration into the CNS is enhanced in WNV-infected *Ccr7*$^{-/-}$ mice. (A) Dot plots of CD8$^+$ T cells (lower right box) and CD4$^+$ T cells (upper left box), after forward scatter/side scatter and UV-negative CD3$^+$ gating, are shown at day 12 postinfection based on flow cytometry analysis from the CNS of WT and *Ccr7*$^{-/-}$ mice. (B, C, and F to I) Following forward scatter/side scatter and UV-negative gating for live cells, total cell numbers of CD8$^+$ T cells (CD3$^+$ CD8$^+$), CD4$^+$ T cells (CD3$^+$ CD4$^+$), inflammatory monocytes (CD45^{hi} Ly6C^{hi} CD11b$^+$), neutrophils (CD45^{hi} Ly6C^{int} CD11b$^+$ Ly6G$^+$; Ly6C^{int} indicates an intermediate expression level of Ly6C), activated CD8$^+$ T cells (CD3$^+$ CD8$^+$ CD44$^+$), and activated CD4$^+$ T cells (CD3$^+$ CD4$^+$ CD44$^+$) were assessed by flow cytometry from the CNS on days 0, 8, and 12 postinfection of WT and *Ccr7*$^{-/-}$ mice. (D) Paraffin-embedded brain sections from WT and *Ccr7*$^{-/-}$ mice on day 12 postinfection were stained for MAC2, myeloperoxidase (MPO), and CD3, and positive cells (shown in brown; indicated by black arrows) are shown within the parenchyma and meninges of WNV-infected mice. Representative images are shown at a magnification of ×20, with zoomed-in insets. (E) Dot plots of inflammatory monocytes (top box) and neutrophils (bottom box), after forward scatter/side scatter and UV-negative CD45^{hi} gating, are shown at day 12 postinfection based on flow cytometry analysis from the CNS of WT and *Ccr7*$^{-/-}$ mice. (J and K) Protein levels of CCL19 and CCL21 from the CNS on days 0, 8, and 12 of WT and *Ccr7*$^{-/-}$ mice were measured by an ELISA. (L and M) Following forward scatter/side scatter and UV-negative gating for live cells, total cell numbers of mDCs (MHC-II^{hi} CD11c$^+$) and Treg cells (CD3$^+$ CD4$^+$ FoxP3$^+$ CD25$^+$) were assessed by flow cytometry from the CNS on day 8 postinfection in WT and *Ccr7*$^{-/-}$ mice. Data are shown as means ± standard deviations for $n = 3$ to 9 mice per genotype and time point from two independent experiments. *, $P < 0.05$; ***, $P < 0.001$.

day 10 (Fig. S2B to H). Together, these data suggest that Ccr7 dampens immunopathology by regulating the production of important proinflammatory mediators.

Given the excessive number of leukocytes infiltrating the CNS and the elevated cytokine production in the absence of Ccr7, we next evaluated the activation/proliferation of astrocytes and microglia, resident immune cells within the CNS that express Ccr7 and are potent producers of cytokines (18, 19). We observed an increase in astrocyte activation of the *Ccr7*$^{-/-}$ mice on day 12, which was observed through increased glial fibrillary acidic protein (GFAP) staining (Fig. 5E). We further confirmed this quantitatively through mRNA expression of GFAP on days 8 and 12 (Fig. 5C), which showed ~6- and ~2-fold increases in the *Ccr7*$^{-/-}$ mice versus WT levels, respectively.

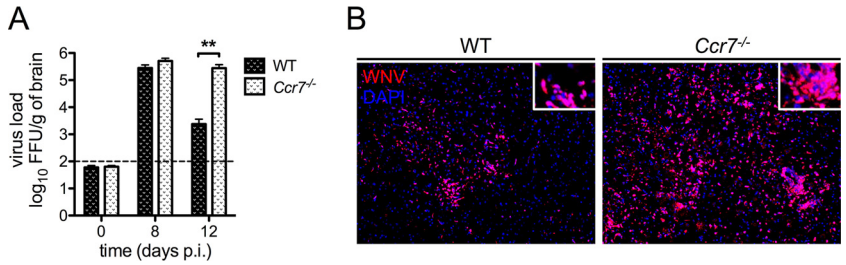

FIG 4 Viral titers are elevated in the CNS of mice deficient for Ccr7. (A) Viral titers were quantified in the brain by FFU assay in WT and *Ccr7*$^{-/-}$ mice. The dotted line indicates the assay's limit of detection. (B) Paraffin-embedded brain sections from WT and *Ccr7*$^{-/-}$ mice on day 12 postinfection were stained for WNV (red) and nuclear 4′,6′-diamidino-2-phenylindole (DAPI; blue). Representative images are shown at a magnification of ×10, with zoomed-in insets. Data are shown as means ± standard deviations for n = 3 to 9 mice per genotype and time point from two independent experiments. **, $P < 0.01$.

We also observed a significant increase in microglial activation (yellow) in *Ccr7*$^{-/-}$ mice, which we visualized through positive costaining for Iba1 (red) and MAC2 (green) by immunofluorescence analysis (Fig. 5F). Because this staining is not specific for microglia, we also evaluated the expression of Cx3cr1, the only resident CNS cell type that expresses this receptor, at the mRNA level in the CNS on days 8 and 12, which was enhanced ~2-fold in WNV-infected *Ccr7*$^{-/-}$ mice and suggests that microglia proliferation was also increased (Fig. 5D). Together, these results suggest that the overall inflammatory response within the CNS is enhanced in the absence of Ccr7.

Ccr7 limits the infiltration of WNV-infected myeloid cells into the CNS. The infiltration of leukocytes into the CNS and the effector capability of T cells to produce IFN-γ have been shown to be important for viral clearance in WNV-infected mice (13, 31, 32). Interestingly, despite the increased T cell accumulation and production of IFN-γ observed in the CNS of *Ccr7*$^{-/-}$ mice, WNV clearance within the CNS was impaired. It

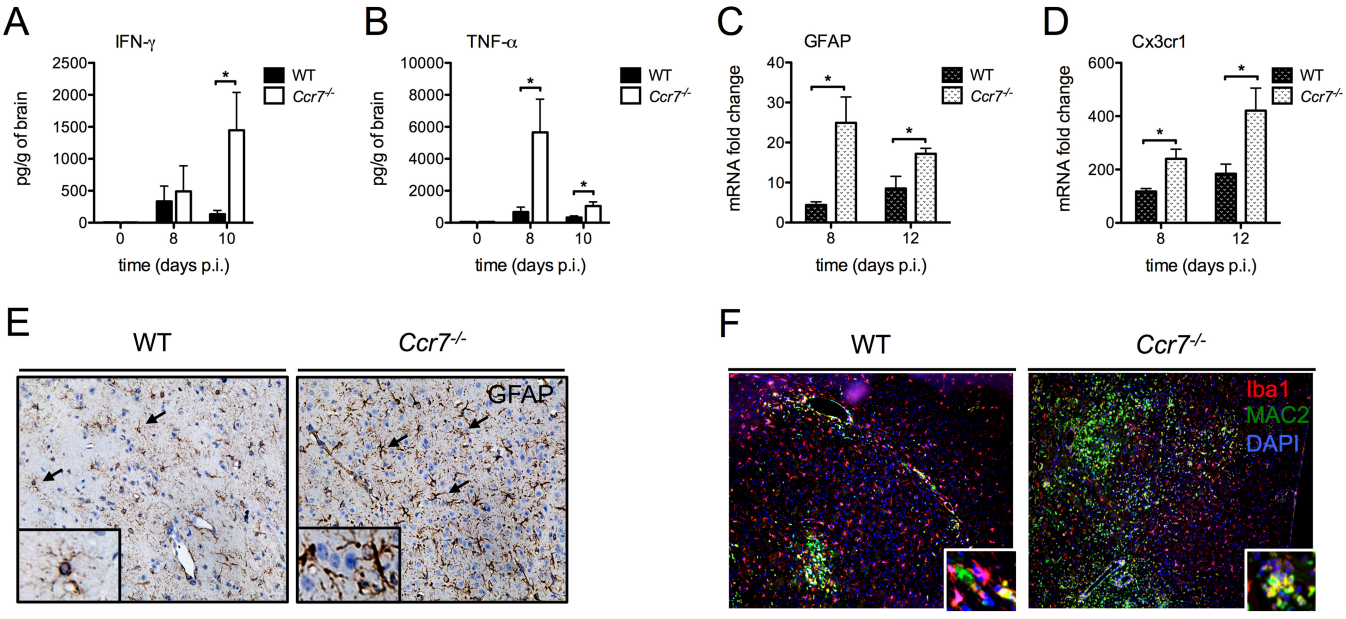

FIG 5 Loss of Ccr7 leads to increased neuroinflammation. (A and B) Protein levels of IFN-γ and TNF-α in the CNS of WT and *Ccr7*$^{-/-}$ mice at days 0, 8, and 10 postinfection were measured by multiplex ELISA. (C and D) Levels of GFAP and Cx3cr1 mRNAs from the CNS of WT and *Ccr7*$^{-/-}$ mice were measured by quantitative RT-PCR. (E) Paraffin-embedded brain sections from WT and *Ccr7*$^{-/-}$ mice on day 12 postinfection were stained for GFAP, and positive cells (shown in brown, indicated by black arrows) are shown within the parenchyma of WNV-infected mice. (F) Paraffin-embedded brain sections from WT and *Ccr7*$^{-/-}$ mice on day 12 postinfection were stained for Iba1 (red), MAC2 (green), and nuclear 4′,6′-diamidino-2-phenylindole (DAPI; blue), and positive cells are shown within the parenchyma of WNV-infected mice. Activated microglia (yellow) costain positive for both Iba1 and MAC2. Representative images are shown at a magnification of ×20, with zoomed-in insets. Data are shown as means ± standard deviations for n = 3 to 9 mice per genotype and time point from two independent experiments. *, $P < 0.05$.

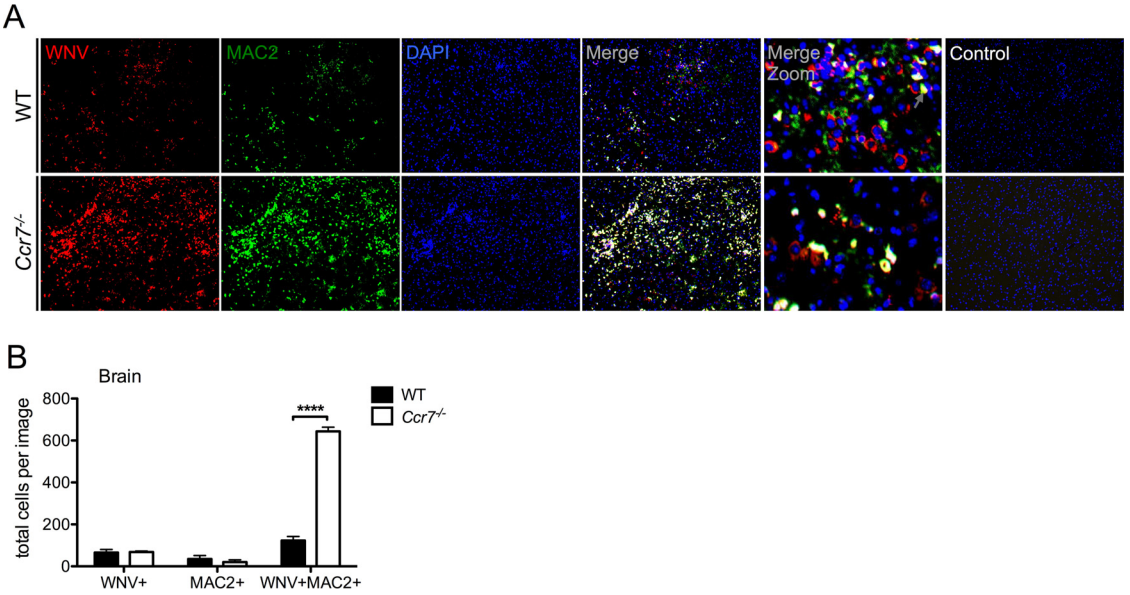

FIG 6 Ccr7 restricts the number of WNV-infected myeloid cells in the CNS. (A) Paraffin-embedded brain sections from WT and *Ccr7*$^{-/-}$ mice on day 12 postinfection were stained for WNV (red), MAC2 (green), and nuclear 4′,6′-diamidino-2-phenylindole (DAPI; blue). WNV-infected myeloid cells costained positive for both WNV and MAC2 and appear in yellow. Control conditions, under which only secondary antibodies were used, are shown. Representative images are shown at a magnification of ×10, with zoomed-in panels. (B) Quantification of single- and double-positive WNV and MAC2 cells from $n = 3$ images per mouse strain in matching brain areas. Data are shown as means ± standard deviations. ****, $P < 0.0001$.

has been proposed that viral entry into the CNS is in part mediated by a Trojan horse mechanism whereby immune cells harbor WNV and traffic the virus into the CNS. As myeloid cells have been implicated in supporting viral replication (33, 34) and serving as a Trojan horse for delivering virus into the CNS (35), we hypothesized that the increased myeloid cells observed in the CNS may be harboring WNV, leading to the observed increased viral load on day 12. To test this hypothesis, we performed immunofluorescence assays to evaluate WNV infection within myeloid cells within the CNS. As shown in Fig. 6A, we observed a striking enhancement of WNV-infected myeloid cells (yellow) in the CNS of *Ccr7*$^{-/-}$ mice in comparison to levels in WT mice, with the majority of viral antigen (red) colocalizing with MAC2 staining (green). Quantification revealed an ~6-fold greater number of positive WNV (red) and MAC2 (green) costained cells in the Ccr7-deficient mice than in WT mice. While colocalization of the two antigens is high in the Ccr7-deficient mice, it is not complete as the levels of WNV and MAC2 single staining were similar between WT and Ccr7-deficient mice (Fig. 6B). Staining of these tissues using secondary antibody alone showed no nonspecific binding. Together, our data suggest that although the loss of Ccr7 results in increased antiviral T cell infiltration into the CNS, viral clearance is still impaired due to the increased number of WNV-infected myeloid cells.

DISCUSSION

One of the most important roles of Ccr7 is the homing of various subpopulations of T cells and DCs to the lymph nodes. In this study, we sought to understand how the loss of this interaction impacted the pathogenesis of WNV. We demonstrate that Ccr7 is essential for controlling viral replication within the CNS and survival following WNV infection. Our data based on the use of Ccr7-deficient mice revealed several fundamental findings regarding viral pathogenesis. First, Ccr7 guides mDCs and T cells into the draining lymph node following WNV infection; however, the loss of this interaction has essentially no impact on T cell activation or the development of WNV antigen-specific T cells. Our findings are similar to those of a study in a murine *Listeria monocytogenes* infection model, where efficient priming of CD8^{+} T cells was found to be Ccr7 independent (36). In contrast in gamma herpesvirus 68–infected mice, a

temporally efficient activation of T cells and viral clearance were Ccr7 dependent (37). Thus, the role of Ccr7 in T cell activation appears to be context and model dependent. Our data align with the notion that Ccr7 does not impact the generation of effector T cells, despite the enormous defect in DC-T cell migration into the lymph node during WNV infection.

A second major finding of our study is that despite the drastic loss of dendritic cell accumulation in the draining lymph node, viral titers at this early site of infection were unaffected, suggesting that the virus is likely entering the draining lymph node through a DC-independent mechanism. This finding was unexpected considering several reports suggesting that virus may reach the draining lymph node through skin dendritic cells (6, 20, 38). In WT mice, Langerhans cells migrate to draining lymph nodes during WNV infection (6, 20). In this study, we did not specifically evaluate Langerhans cells, but Langerhans cells would have been captured within the mDC (MHC-II^{hi} CD11c^{+}) population that was measured in the current study (Fig. 1B), which shows that MHC-II^{hi} CD11c^{+} cells are nearly ablated throughout the course of infection in Ccr7-deficient mice. Therefore, Langerhans cells would also be nearly absent from the draining lymph node during infection as well. Indeed, Langerhans cells require Ccr7 to migrate into lymph nodes (39), and during homeostasis and inflammatory conditions, Langerhans cells are absent in the draining lymph node in Ccr7-deficient mice (17, 40–42). Therefore, the current evidence indicates that Langerhans cells would be an unlikely source of viral trafficking to the draining lymph nodes in our study. Regardless, our studies demonstrate that viral entry and replication in lymph nodes immediately following infection occur with equal efficiency even when the vast majority of the DCs are absent. Our data suggest that WNV likely enters into the draining lymph nodes through an alternative route, possibly hematogenously.

A third interesting finding from our study is that in the absence of Ccr7, leukocytes were no longer retained in the lymph nodes, resulting in an immediate leukocytosis that was sustained through much of the infection. Subsequently, this leukocytosis, along with elevated chemokine production in the CNS, may have promoted the excessive migration of these leukocytes into the CNS. This suggests that the bioavailability of leukocytes in the blood may be a major contributing factor that determines the number of leukocytes capable of reaching the CNS. This has previously been shown to be the case for inflammatory monocytes, where the number of monocytes migrating into the CNS was controlled primarily by how many had been mobilized into the blood (43, 44). The enhanced pan-leukocyte infiltration into the CNS during WNV infection was reminiscent of the phenotype observed in the absence of IL-1β signaling, where WNV-infected *Il-1r*$^{-/-}$ mice also presented with a significant increase in leukocyte infiltration and overproduction of inflammatory cytokines in the CNS (45). Taken together, our results show that Ccr7 is responsible for leukocyte retention in the lymph nodes, which restricts leukocytosis and limits leukocyte entry into the CNS. As chemokines involved in recruiting leukocytes are elevated in the blood of Ccr7-deficient mice, this may also be contributing to the pan-leukocytosis event observed. In addition to a possible defect in the retention of T cells in the lymph nodes, a defect in the retention of monocytes and neutrophils from the bone marrow cannot be excluded. Another plausible scenario is that viral infection may be enhanced in the periphery of Ccr7-deficient mice in organs not tested here. However, this does not appear to be the case during the early stages of infection of the blood, lymph nodes, and spleen as viral titers are similar between WT and Ccr7-deficient mice.

Equally open to further investigation is the possibility that Ccr7 restricts the activation and proliferation of microglia and astrocytes within the brain itself. At the steady state, microglia perform continuous surveillance of the CNS for danger signals and provide trophic support to neurons (46). When activated, microglia proliferate, form nodules to surround areas of damage, and secrete cytokines/chemokines to recruit immune cells (47–53). Despite different triggering events, microglia activation is a major characteristic of neurodegenerative conditions, including Alzheimer's disease,

Parkinson's diseases, traumatic brain injury, and multiple sclerosis (54–57). Similarly, when activated, astrocytes proliferate and are potent producers of cytokines/chemokines (51). Our data show that there is an increase in microglia and astrocytes in the absence of Ccr7, as well as an excess of cytokines/chemokines and leukocyte infiltrates. Thus, while an effective immune response is necessary for viral clearance in the CNS, an excessive response can induce tissue injury as the CNS is an immune-privileged organ (58). $CD8^+$ T cell recruitment to the CNS is required for effective viral clearance during WNV infection; however, virus-specific versus bystander $CD8^+$ T cell accumulation in the CNS can differentially activate glial cells, leading to neuronal death (14, 59). Furthermore, excessive IFN-γ levels in the brain are associated with neuroinflammation in models of pathogenic infections and autoimmunity (60–66). Thus, a hyperreactive immune response in the CNS is most likely contributing to the excessive cell death observed in Ccr7-deficient mice.

Last, Ccr7 may contribute to effective viral clearance through the restriction of monocyte/macrophage cell entry into the CNS as we have demonstrated that mice lacking Ccr7 have elevated numbers of myeloid cells in the CNS that also costain for WNV. These myeloid cells may be monocytes/macrophages carrying WNV into the CNS or supporting viral replication once in the CNS. WNV infection of mDCs occurs in both humans and mice (7, 67–72). Indeed the excess infiltration/rate of replication of WNV-infected myeloid cells and subsequent cytokine storm could be outcompeting the rate of viral clearance by immune cells. Virologic control could also be impaired through the excess effector functions of the infiltrating immune cells as there is an excess in the number of infiltrating immune cells and in cytokine production in Ccr7-deficient mice. It cannot be excluded that microglia are also supporting viral replication as MAC2 is a pan-myeloid cell maker. However, it has been shown that neurons are the primary CNS-resident cell type that supports WNV replication in the CNS (10). It has been shown that monocytes/macrophages do support viral replication and perhaps act via a Trojan horse mechanism to bring virus into the CNS during WNV infection (33–35), an observation which supports our data. The role of monocytes/macrophages has been shown to be protective during WNV infection: when these cells are depleted via clodronate-loaded liposomes or when they are largely absent from the CNS through the use of *Ccr2*$^{-/-}$ mice, encephalitis is greatly enhanced in mice (44, 73, 74). However, our studies demonstrate that efforts to promote monocytes/macrophages into the CNS may be detrimental as these may increase the shuttling of virus-infected cells. Thus, immunomodulatory strategies aimed at promoting monocyte migration in the CNS should consider this possibility. Future studies aimed at targeted deletion of Ccr7 in a cellular specific or tissue-specific manner will also provide much needed insight into the pleiotropic function behind the unusual biology of this receptor. Together, our data demonstrate that Ccr7 is critical for regulating neuroinflammation and provide novel insight into the role of Ccr7 in coordinating the immune response during WNV infection *in vivo*.

MATERIALS AND METHODS

WNV infection model. Mouse studies were carried out in an animal biosafety level 3 facility under a protocol approved by the Icahn School of Medicine at Mount Sinai Animal Care and Use Committee. C57BL/6J mice were purchased from The Jackson Laboratory; congenic *Ccr7*$^{-/-}$ mice were backcrossed on the C57BL/6J background for 10 generations by Sergio Lira (75). In all experiments, Ccr7-deficient mice were compared with their corresponding wild-type (WT) littermates. Female mice 8 to 12 weeks old were footpad injected with 10^4 focus forming units (FFU) of WNV-NY99 (provided by Alexander Pletnev) in 20 μl of phosphate-buffered saline (PBS) or with PBS alone (mock infection).

Viral titers. Titers of WNV were determined on Vero cell monolayers as previously described (43). Briefly, 150 μl of virus-containing material was adsorbed for 1 h at 37°C in 24-well plates, and cells were overlaid with 1 ml of Opti-MEM (Invitrogen) supplemented with 0.8% methyl cellulose, 2% fetal bovine serum (FBS), and 50 μg/ml gentamicin sulfate. Cells were incubated for 2 days at 37°C, fixed with 100% methanol, and incubated for 1 h at 37°C with 500 μl of a 1:5,000 dilution of WNV E24 antibodies (BEI Resources). Anti-mouse horseradish peroxidase-labeled polymer (1:10 μl) (DakoCytomation) was added. WNV foci were visualized by the addition of 1 ml of diaminobenzidine chromogen.

RNA extraction and quantitative RT-PCR. RNA was extracted from brain, lymph nodes, and blood using TRIzol (Invitrogen); for viral RNA, Qiagen's Viral RNA minikit (Qiagen) was used. RNA (150 ng) was

converted to cDNA using a Superscript III Supermix kit (Invitrogen) with random hexamers. Real-time PCR (RT-PCR) was performed using TaqMan PCR Master mix (Applied Biosciences) and the following primers (Applied Biosystems Inc.): NS5 forward, 5′-ACCACGGCAGTTATGATGTGAAG-3′; NS5 reverse, 5′-CACTCC ATTGACCAGCGAACT-3′; 6-carboxyfluorescein (FAM)-labeled probe, 5′-CCCACAGGCTCCGCC-3′; Cx3cr1 forward, 5′-AGGTCCCTGTCATGCTTCTG-3′; Cx3cr1 reverse, 5′-TCTGGACCCATTCCTTCTTG-3′; GFAP forward, 5′-CGTGTGGATTTGGAGAGAAAG-3′; GFAP reverse, 5′-GTGAGGTCTGCAAACTTAGACC-3′; glyceraldehyde-3-phosphate dehydrogenase (GAPDH) forward, 5′-AACTTTGGCATTGTGGAAGG-3′; and GAPDH reverse, 5′-ACACATTGGGGGTAGGAACA-3′. All reactions were run using a Roche LightCycler 480 Real Time PCR System. Calculated copies were normalized against the number of copies of the housekeeping gene GAPDH, and fold increase was determined using the $\Delta\Delta C_T$ (where C_T is threshold cycle) method. For viral RNA, copy number was calculated by fitting observed C_T values to the slope of a standardized curve generated using a WNV NS5-containing plasmid.

Cell isolation. Brains were collected aseptically in 7 ml of fluorescence-activated cell sorting (FACS) buffer (PBS–2% FBS) and homogenized using a Dounce homogenizer. After the addition of 3 ml of 100% isotonic Percoll (GE Healthcare), the homogenate was underlaid with 1 ml of 70% isotonic Percoll. After centrifugation at 2,470 rpm for 30 min at 4°C, cells at the interphase were isolated and washed in FACS buffer. A total of 200 μl of anticoagulated blood was incubated with PharmLyse buffer (BD Biosciences) to remove erythrocytes. Lymph nodes and spleens were mechanically homogenized in digestion buffer (1.67 Wünsch units/ml Liberase TL [thermolysin low] Research Grade enzyme and 0.2 mg/ml DNase I [both, Roche Diagnostics] in RPMI 1640 medium) for 5 min (lymph nodes) or 20 min (spleens) at 37°C to generate a single-cell suspension.

Flow cytometry. Following isolation of organs into single-cell suspensions, cells were stained with antibodies and Live/Dead Fixable Blue Dead Cell Stain (Invitrogen). The following antibodies were used: fluorescein isothiocyanate (FITC)-conjugated Ly6C (clone AL-21; BD Biosciences), CD3 (clone 17A2; BD Biosciences), and CD8 (clone 53.6.7; eBiosciences); phycoerythrin (PE)-conjugated CD45 (clone 30-F11; eBiosciences); peridinin chlorophyll protein (PerCP)-Cy5.5-conjugated Ly6G (clone 1A8; BD Biosciences) and CD3 (clone 17A2; BD Biosciences); allophycocyanin (APC)-Cy7-conjugated CD11b (clone M1/70; BD Biosciences), CD4 (clone RM4-5; eBiosciences) CD44 (clone IM7; eBiosciences), and CD11c (clone N18; eBiosciences); PE-Cy7-conjugated MHC-II (clone M5/114.15.2; eBiosciences). Data were collected on an LSR II instrument (Becton-Dickinson), and analysis was performed using FlowJo software, version 8.5.3 (TreeStar). Cell numbers were quantified using counting beads (Spherotech, Inc.).

Protein quantification. Cytokine and chemokine protein concentrations were determined using a multiplex enzyme-linked immunosorbent assay (ELISA). Antibodies and cytokine standards were purchased from R&D Systems or Peprotech, and individual Luminex bead regions were coupled to capture antibodies for each cytokine or chemokine measured, as previously described (76). The plates were read on a Luminex Magpix platform. The median fluorescence intensity for each region was determined using the Milliplex software and a five-parameter regression algorithm. Cytokine levels were measured using ELISA kits according to the manufacturer's instructions. A mouse CCL19 ELISA kit (DY440) and mouse CCL21 (DY4570) DuoSet ELISA were purchased from R&D Systems.

Intracellular cytokine staining. A total of 10^6 splenocytes were stimulated with 0.2 μg/ml immunodominant D^b-restricted WNV-specific NS4B peptide (SSVWNATTAI) (BEI Resources) for 6 h at 37°C, with the addition of brefeldin A (1 μg/ml; BD Biosciences). Cells for IFN-γ/TNF-α, IL-17A, and regulatory T (Treg) cell staining were then incubated with Fc block (1:200; BD Biosciences), surface antibodies, and Live/Dead Fixable Blue Dead Cell Stain (Invitrogen) for 30 min at 4°C. Cells were fixed and permeabilized with 200 μl of Cytofix/Cytoperm (BD Biosciences) prior to staining with intracellular antibodies for 30 min at 4°C. The following antibodies were used: PE-conjugated IFN-γ (clone XMG1.2; BD Biosciences) and FoxP3 (clone FJK-16S; eBiosciences); PerCP-Cy5.5-conjugated IL-17A (clone 17B7; eBiosciences) and CD3 (clone 17A2; eBiosciences); PE-Cy5.5-conjugated TNF-α (clone MP6-XT22; BD Biosciences); FITC-conjugated CD8 (clone 53.6.7; eBiosciences) and CD3 (clone 17A2; eBiosciences); APC-Cy7-conjugated CD4 (clone RM4-5; eBiosciences); APC-conjugated CD25 (clone PC61.5; eBiosciences).

Tissue sectioning and staining. Tissues were fixed with 4% paraformaldehyde. Immunohistochemistry was performed with serial 6-μm paraffin-embedded sections. After rehydration, antigen retrieval was performed using 10 mM citrate buffer at pH 6, as previously described (43). For monocyte/macrophage staining, slides were blocked for 1 h at room temperature and stained with rat anti-mouse MAC2 antibody (1:200; BioLegend) in Dako background reducing diluent. Slides were incubated with 2.5 μg/ml biotinylated anti-rat IgG antibody (Southern Biotech) and incubated for 30 min with Vectastain Elite ABC-peroxidase reagent (Vector Laboratories). Staining for CD3 (1:100; Vector Laboratories), myeloperoxidase (1:500; Dako), and GFAP (1:500; Dako) was performed in conjunction with a rabbit EnVision+/HRP kit (Dako), according to the manufacturer's instructions. All immunohistochemistry staining was visualized by incubating sections with 3,3′-diaminobenzidine substrate for 1 to 2 min and counterstaining with hematoxylin. To visualize WNV, Iba1, and MAC2 fluorescence staining, slides were incubated overnight with mouse ascites fluid (1:100), rabbit anti-Iba1 antibody (1:500; Wako Chemicals, USA), or rat anti-MAC2 antibody (1:100; Cedarlane Labs), respectively. Slides were incubated for 40 min in Alexa Fluor 555 goat anti-mouse antibody, Alexa Fluor 594 donkey anti-rabbit antibody, Alexa Fluor 488 goat anti-rat antibody, or Alexa Fluor 488 donkey anti-rat antibody (1:200; Jackson ImmunoResearch Laboratories). All slides were analyzed using an AxioImager Z2 microscope (Zeiss) and Zen 2012 software (Zeiss).

Statistical analysis. All data were assessed for statistical significance with Prism, version 5.0f, software (GraphPad Software). Differences in cytokine levels and viral burden were analyzed by a Mann-Whitney *U* test, and differences in cell numbers were analyzed by a Student's unpaired *t* test.

Kaplan-Meier survival curves were analyzed by the log rank test. *P* values indicating statistical significance are given in the figure legends.

SUPPLEMENTAL MATERIAL

Supplemental material for this article may be found at https://doi.org/10.1128/JVI.02409-16.

SUPPLEMENTAL FILE 1, PDF file, 0.3 MB.

ACKNOWLEDGMENTS

We thank the Flow Cytometry Shared Resource Facility, Center for Comparative Medicine and Surgery, Microscopy CoRE, at the Icahn School of Medicine at Mount Sinai for technical assistance and Dusan Bogunovic for critical readings of the manuscript.

S.V.B and J.K.L. conceived and designed the experiments and wrote the manuscript; S.V.B, D.M., K.W.H., J.A.B., J.S., and J.K.L. conducted the experiments, assembled and analyzed the data, and interpreted the results; A.G.P. and S.A.L. provided technical assistance and key reagents.

This work was funded in part by NIAID grant R01AI108715 (J.K.L), the Division of Intramural Research, NIAID, NIH (A.G.P.), an NIH Research Training Award T32AI007647 (S.V.B), and NIAID grant F31AI110071 (S.V.B). The funders had no role in study design, data collection and interpretation, or the decision to submit the work for publication.

We declare that we have no conflicts of interest or competing financial interests.

REFERENCES

1. Gubler DJ. 2007. The continuing spread of West Nile virus in the western hemisphere. Clin Infect Dis 45:1039–1046. https://doi.org/10.1086/521911.
2. Petersen LR, Roehrig JT. 2001. West Nile virus: a reemerging global pathogen. Emerg Infect Dis 7:611–614. https://doi.org/10.3201/eid0704.017401.
3. Omalu BI, Shakir AA, Wang G, Lipkin WI, Wiley CA. 2003. Fatal fulminant pan-meningo-polioencephalitis due to West Nile virus. Brain Pathol 13:465–472.
4. Armah HB, Wang G, Omalu BI, Tesh RB, Gyure KA, Chute DJ, Smith RD, Dulai P, Vinters HV, Kleinschmidt-DeMasters BK, Wiley CA. 2007. Systemic distribution of West Nile virus infection: postmortem immunohistochemical study of six cases. Brain Pathol 17:354–362. https://doi.org/10.1111/j.1750-3639.2007.00080.x.
5. Busch MP, Wright DJ, Custer B, Tobler LH, Stramer SL, Kleinman SH, Prince HE, Bianco C, Foster G, Petersen LR, Nemo G, Glynn SA. 2006. West Nile virus infections projected from blood donor screening data, United States, 2003. Emerg Infect Dis 12:395–402. https://doi.org/10.3201/eid1205.051287.
6. Byrne SN, Halliday GM, Johnston LJ, King NJ. 2001. Interleukin-1β but not tumor necrosis factor is involved in West Nile virus-induced Langerhans cell migration from the skin in C57BL/6 mice. J Investig Dermatol 117:702–709. https://doi.org/10.1046/j.0022-202x.2001.01454.x.
7. Silva MC, Guerrero-Plata A, Gilfoy FD, Garofalo RP, Mason PW. 2007. Differential activation of human monocyte-derived and plasmacytoid dendritic cells by West Nile virus generated in different host cells. J Virol 81:13640–13648. https://doi.org/10.1128/JVI.00857-07.
8. Lim PY, Behr MJ, Chadwick CM, Shi PY, Bernard KA. 2011. Keratinocytes are cell targets of West Nile virus in vivo. J Virol 85:5197–5201. https://doi.org/10.1128/JVI.02692-10.
9. Eldadah AH, Nathanson N, Sarsitis R. 1967. Pathogenesis of West Nile Virus encephalitis in mice and rats. 1. Influence of age and species on mortality and infection. Am J Epidemiol 86:765–775.
10. Shrestha B, Gottlieb D, Diamond MS. 2003. Infection and injury of neurons by West Nile encephalitis virus. J Virol 77:13203–13213. https://doi.org/10.1128/JVI.77.24.13203-13213.2003.
11. Glass WG, McDermott DH, Lim JK, Lekhong S, Yu SF, Frank WA, Pape J, Cheshier RC, Murphy PM. 2006. CCR5 deficiency increases risk of symptomatic West Nile virus infection. J Exp Med 203:35–40. https://doi.org/10.1084/jem.20051970.
12. Purtha WE, Myers N, Mitaksov V, Sitati E, Connolly J, Fremont DH, Hansen TH, Diamond MS. 2007. Antigen-specific cytotoxic T lymphocytes protect against lethal West Nile virus encephalitis. Eur J Immunol 37:1845–1854. https://doi.org/10.1002/eji.200737192.
13. Shrestha B, Samuel MA, Diamond MS. 2006. CD8$^+$ T cells require perforin to clear West Nile virus from infected neurons. J Virol 80:119–129. https://doi.org/10.1128/JVI.80.1.119-129.2006.
14. Shrestha B, Diamond MS. 2004. Role of CD8$^+$ T cells in control of West Nile virus infection. J Virol 78:8312–8321. https://doi.org/10.1128/JVI.78.15.8312-8321.2004.
15. Beauvillain C, Cunin P, Doni A, Scotet M, Jaillon S, Loiry ML, Magistrelli G, Masternak K, Chevailler A, Delneste Y, Jeannin P. 2011. CCR7 is involved in the migration of neutrophils to lymph nodes. Blood 117:1196–1204. https://doi.org/10.1182/blood-2009-11-254490.
16. Forster R, Davalos-Misslitz AC, Rot A. 2008. CCR7 and its ligands: balancing immunity and tolerance. Nat Rev Immunol 8:362–371. https://doi.org/10.1038/nri2297.
17. Forster R, Schubel A, Breitfeld D, Kremmer E, Renner-Muller I, Wolf E, Lipp M. 1999. CCR7 coordinates the primary immune response by establishing functional microenvironments in secondary lymphoid organs. Cell 99:23–33. https://doi.org/10.1016/S0092-8674(00)80059-8.
18. Gomez-Nicola D, Pallas-Bazarra N, Valle-Argos B, Nieto-Sampedro M. 2010. CCR7 is expressed in astrocytes and upregulated after an inflammatory injury. J Neuroimmunol 227:87–92. https://doi.org/10.1016/j.jneuroim.2010.06.018.
19. Dijkstra IM, de Haas AH, Brouwer N, Boddeke HW, Biber K. 2006. Challenge with innate and protein antigens induces CCR7 expression by microglia in vitro and in vivo. Glia 54:861–872. https://doi.org/10.1002/glia.20426.
20. Johnston LJ, Halliday GM, King NJ. 2000. Langerhans cells migrate to local lymph nodes following cutaneous infection with an arbovirus. J Investig Dermatol 114:560–568. https://doi.org/10.1046/j.1523-1747.2000.00904.x.
21. Tsou CL, Peters W, Si Y, Slaymaker S, Aslanian AM, Weisberg SP, Mack M, Charo IF. 2007. Critical roles for CCR2 and MCP-3 in monocyte mobilization from bone marrow and recruitment to inflammatory sites. J Clin Invest 117:902–909. https://doi.org/10.1172/JCI29919.
22. Jia T, Serbina NV, Brandl K, Zhong MX, Leiner IM, Charo IF, Pamer EG. 2008. Additive roles for MCP-1 and MCP-3 in CCR2-mediated recruitment of inflammatory monocytes during Listeria monocytogenes infection. J Immunol 180:6846–6853. https://doi.org/10.4049/jimmunol.180.10.6846.
23. Hou W, Kang HS, Kim BS. 2009. Th17 cells enhance viral persistence and inhibit T cell cytotoxicity in a model of chronic virus infection. J Exp Med 206:313–328. https://doi.org/10.1084/jem.20082030.
24. Singh RP, Hasan S, Sharma S, Nagra S, Yamaguchi DT, Wong DT, Hahn

BH, Hossain A. 2014. Th17 cells in inflammation and autoimmunity. Autoimmun Rev 13:1174–1181. https://doi.org/10.1016/j.autrev.2014.08.019.
25. Christiaansen AF, Knudson CJ, Weiss KA, Varga SM. 2014. The CD4 T cell response to respiratory syncytial virus infection. Immunol Res 59:109–117. https://doi.org/10.1007/s12026-014-8540-1.
26. Wang Q, Zhou J, Zhang B, Tian Z, Tang J, Zheng Y, Huang Z, Tian Y, Jia Z, Tang Y, van Velkinburgh JC, Mao Q, Bian X, Ping Y, Ni B, Wu Y. 2013. Hepatitis B virus induces IL-23 production in antigen presenting cells and causes liver damage via the IL-23/IL-17 axis. PLoS Pathog 9:e1003410. https://doi.org/10.1371/journal.ppat.1003410.
27. Welte T, Aronson J, Gong B, Rachamallu A, Mendell N, Tesh R, Paessler S, Born WK, O'Brien RL, Wang T. 2011. Vγ4$^+$ T cells regulate host immune response to West Nile virus infection. FEMS Immunol Med Microbiol 63:183–192. https://doi.org/10.1111/j.1574-695X.2011.00840.x.
28. Lanteri MC, O'Brien KM, Purtha WE, Cameron MJ, Lund JM, Owen RE, Heitman JW, Custer B, Hirschkorn DF, Tobler LH, Kiely N, Prince HE, Ndhlovu LC, Nixon DF, Kamel HT, Kelvin DJ, Busch MP, Rudensky AY, Diamond MS, Norris PJ. 2009. Tregs control the development of symptomatic West Nile virus infection in humans and mice. J Clin Invest 119:3266–3277.
29. Wang Y, Lobigs M, Lee E, Mullbacher A. 2003. CD8$^+$ T cells mediate recovery and immunopathology in West Nile virus encephalitis. J Virol 77:13323–13334. https://doi.org/10.1128/JVI.77.24.13323-13334.2003.
30. Durrant DM, Robinette ML, Klein RS. 2013. IL-1R1 is required for dendritic cell-mediated T cell reactivation within the CNS during West Nile virus encephalitis. J Exp Med 210:503–516. https://doi.org/10.1084/jem.20121897.
31. Shrestha B, Wang T, Samuel MA, Whitby K, Craft J, Fikrig E, Diamond MS. 2006. Gamma interferon plays a crucial early antiviral role in protection against West Nile virus infection. J Virol 80:5338–5348. https://doi.org/10.1128/JVI.00274-06.
32. Lim JK, Murphy PM. 2011. Chemokine control of West Nile virus infection. Exp Cell Res 317:569–574. https://doi.org/10.1016/j.yexcr.2011.01.009.
33. Garcia-Tapia D, Loiacono CM, Kleiboeker SB. 2006. Replication of West Nile virus in equine peripheral blood mononuclear cells. Vet Immunol Immunopathol 110:229–244. https://doi.org/10.1016/j.vetimm.2005.10.003.
34. Rios M, Zhang MJ, Grinev A, Srinivasan K, Daniel S, Wood O, Hewlett IK, Dayton AI. 2006. Monocytes-macrophages are a potential target in human infection with West Nile virus through blood transfusion. Transfusion 46:659–667. https://doi.org/10.1111/j.1537-2995.2006.00769.x.
35. Dai J, Wang P, Bai F, Town T, Fikrig E. 2008. ICAM-1 participates in the entry of West Nile virus into the central nervous system. J Virol 82:4164–4168. https://doi.org/10.1128/JVI.02621-07.
36. Kursar M, Hopken UE, Koch M, Kohler A, Lipp M, Kaufmann SH, Mittrucker HW. 2005. Differential requirements for the chemokine receptor CCR7 in T cell activation during *Listeria monocytogenes* infection. J Exp Med 201:1447–1457. https://doi.org/10.1084/jem.20041204.
37. Kocks JR, Adler H, Danzer H, Hoffmann K, Jonigk D, Lehmann U, Forster R. 2009. Chemokine receptor CCR7 contributes to a rapid and efficient clearance of lytic murine gamma-herpes virus 68 from the lung, whereas bronchus-associated lymphoid tissue harbors virus during latency. J Immunol 182:6861–6869. https://doi.org/10.4049/jimmunol.0801826.
38. Welte T, Reagan K, Fang H, Machain-Williams C, Zheng X, Mendell N, Chang GJ, Wu P, Blair CD, Wang T. 2009. Toll-like receptor 7-induced immune response to cutaneous West Nile virus infection. J Gen Virol 90:2660–2668. https://doi.org/10.1099/vir.0.011783-0.
39. Villablanca EJ, Mora JR. 2008. A two-step model for Langerhans cell migration to skin-draining LN. Eur J Immunol 38:2975–2980. https://doi.org/10.1002/eji.200838919.
40. Ohl L, Mohaupt M, Czeloth N, Hintzen G, Kiafard Z, Zwirner J, Blankenstein T, Henning G, Forster R. 2004. CCR7 governs skin dendritic cell migration under inflammatory and steady-state conditions. Immunity 21:279–288. https://doi.org/10.1016/j.immuni.2004.06.014.
41. MartIn-Fontecha A, Sebastiani S, Hopken UE, Uguccioni M, Lipp M, Lanzavecchia A, Sallusto F. 2003. Regulation of dendritic cell migration to the draining lymph node: impact on T lymphocyte traffic and priming. J Exp Med 198:615–621. https://doi.org/10.1084/jem.20030448.
42. Vander Lugt B, Tubo NJ, Nizza ST, Boes M, Malissen B, Fuhlbrigge RC, Kupper TS, Campbell JJ. 2013. CCR7 plays no appreciable role in trafficking of central memory CD4 T cells to lymph nodes. J Immunol 191:3119–3127. https://doi.org/10.4049/jimmunol.1200938.
43. Bardina SV, Michlmayr D, Hoffman KW, Obara CJ, Sum J, Charo IF, Lu W, Pletnev AG, Lim JK. 2015. Differential roles of chemokines CCL2 and CCL7 in monocytosis and leukocyte migration during West Nile virus infection. J Immunol 195:4306–4318. https://doi.org/10.4049/jimmunol.1500352.
44. Lim JK, Obara CJ, Rivollier A, Pletnev AG, Kelsall BL, Murphy PM. 2011. Chemokine receptor Ccr2 is critical for monocyte accumulation and survival in West Nile virus encephalitis. J Immunol 186:471–478. https://doi.org/10.4049/jimmunol.1003003.
45. Ramos HJ, Lanteri MC, Blahnik G, Negash A, Suthar MS, Brassil MM, Sodhi K, Treuting PM, Busch MP, Norris PJ, Gale M, Jr. 2012. IL-1β signaling promotes CNS-intrinsic immune control of West Nile virus infection. PLoS Pathog 8:e1003039. https://doi.org/10.1371/journal.ppat.1003039.
46. Tremblay ME, Stevens B, Sierra A, Wake H, Bessis A, Nimmerjahn A. 2011. The role of microglia in the healthy brain. J Neurosci 31:16064–16069. https://doi.org/10.1523/JNEUROSCI.4158-11.2011.
47. Jang H, Boltz D, McClaren J, Pani AK, Smeyne M, Korff A, Webster R, Smeyne RJ. 2012. Inflammatory effects of highly pathogenic H5N1 influenza virus infection in the CNS of mice. J Neurosci 32:1545–1559. https://doi.org/10.1523/JNEUROSCI.5123-11.2012.
48. Mishra MK, Basu A. 2008. Minocycline neuroprotects, reduces microglial activation, inhibits caspase 3 induction, and viral replication following Japanese encephalitis. J Neurochem 105:1582–1595. https://doi.org/10.1111/j.1471-4159.2008.05238.x.
49. Chauhan VS, Furr SR, Sterka DG, Jr, Nelson DA, Moerdyk-Schauwecker M, Marriott I, Grdzelishvili VZ. 2010. Vesicular stomatitis virus infects resident cells of the central nervous system and induces replication-dependent inflammatory responses. Virology 400:187–196. https://doi.org/10.1016/j.virol.2010.01.025.
50. Chen CJ, Ou YC, Chang CY, Pan HC, Lin SY, Liao SL, Raung SL, Chen SY, Chang CJ. 2011. Src signaling involvement in Japanese encephalitis virus-induced cytokine production in microglia. Neurochem Int 58:924–933. https://doi.org/10.1016/j.neuint.2011.02.022.
51. Das S, Mishra MK, Ghosh J, Basu A. 2008. Japanese encephalitis virus infection induces IL-18 and IL-1β in microglia and astrocytes: correlation with in vitro cytokine responsiveness of glial cells and subsequent neuronal death. J Neuroimmunol 195:60–72. https://doi.org/10.1016/j.jneuroim.2008.01.009.
52. Wang G, Zhang J, Li W, Xin G, Su Y, Gao Y, Zhang H, Lin G, Jiao X, Li K. 2008. Apoptosis and proinflammatory cytokine responses of primary mouse microglia and astrocytes induced by human H1N1 and avian H5N1 influenza viruses. Cell Mol Immunol 5:113–120. https://doi.org/10.1038/cmi.2008.14.
53. Esen N, Blakely PK, Rainey-Barger EK, Irani DN. 2012. Complexity of the microglial activation pathways that drive innate host responses during lethal alphavirus encephalitis in mice. ASN Neuro 4:207–221. https://doi.org/10.1042/AN20120016.
54. Crehan H, Hardy J, Pocock J. 2012. Microglia, Alzheimer's disease, and complement. Int J Alzheimers Dis 2012:983640. https://doi.org/10.1155/2012/983640.
55. Sugama S, Takenouchi T, Cho BP, Joh TH, Hashimoto M, Kitani H. 2009. Possible roles of microglial cells for neurotoxicity in clinical neurodegenerative diseases and experimental animal models. Inflamm Allergy Drug Targets 8:277–284. https://doi.org/10.2174/187152809789352249.
56. Frank-Cannon TC, Alto LT, McAlpine FE, Tansey MG. 2009. Does neuroinflammation fan the flame in neurodegenerative diseases? Mol Neurodegener 4:47. https://doi.org/10.1186/1750-1326-4-47.
57. Rogers J, Mastroeni D, Leonard B, Joyce J, Grover A. 2007. Neuroinflammation in Alzheimer's disease and Parkinson's disease: are microglia pathogenic in either disorder? Int Rev Neurobiol 82:235–246. https://doi.org/10.1016/S0074-7742(07)82012-5.
58. Ransohoff RM, Kivisakk P, Kidd G. 2003. Three or more routes for leukocyte migration into the central nervous system. Nat Rev Immunol 3:569–581. https://doi.org/10.1038/nri1130.
59. Dheen ST, Kaur C, Ling EA. 2007. Microglial activation and its implications in the brain diseases. Curr Med Chem 14:1189–1197. https://doi.org/10.2174/092986707780597961.
60. Meissner N, Swain S, McInnerney K, Han S, Harmsen AG. 2010. Type-I IFN signaling suppresses an excessive IFN-gamma response and thus prevents lung damage and chronic inflammation during pneumocystis (PC) clearance in CD4 T cell-competent mice. Am J Pathol 176:2806–2818. https://doi.org/10.2353/ajpath.2010.091158.
61. Davidson S, Maini MK, Wack A. 2015. Disease-promoting effects of type

I interferons in viral, bacterial, and coinfections. J Interferon Cytokine Res 35:252–264. https://doi.org/10.1089/jir.2014.0227.
62. Ostler T, Davidson W, Ehl S. 2002. Virus clearance and immunopathology by CD8$^+$ T cells during infection with respiratory syncytial virus are mediated by IFN-γ. Eur J Immunol 32:2117–2123. https://doi.org/10.1002/1521-4141(200208)32:8<2117::AID-IMMU2117>3.0.CO;2-C.
63. Schwarting A, Wada T, Kinoshita K, Tesch G, Kelley VR. 1998. IFN-γ receptor signaling is essential for the initiation, acceleration, and destruction of autoimmune kidney disease in MRL-*Fas^{lpr}* mice. J Immunol 161:494–503.
64. Hu X, Ivashkiv LB. 2009. Cross-regulation of signaling pathways by interferon-gamma: implications for immune responses and autoimmune diseases. Immunity 31:539–550. https://doi.org/10.1016/j.immuni.2009.09.002.
65. Mitchell AJ, Yau B, McQuillan JA, Ball HJ, Too LK, Abtin A, Hertzog P, Leib SL, Jones CA, Gerega SK, Weninger W, Hunt NH. 2012. Inflammasome-dependent IFN-γ drives pathogenesis in *Streptococcus pneumoniae* meningitis. J Immunol 189:4970–4980. https://doi.org/10.4049/jimmunol.1201687.
66. Deczkowska A, Baruch K, Schwartz M. 2016. Type I/II interferon balance in the regulation of brain physiology and pathology. Trends Immunol 37:181–192. https://doi.org/10.1016/j.it.2016.01.006.
67. Lazear HM, Lancaster A, Wilkins C, Suthar MS, Huang A, Vick SC, Clepper L, Thackray L, Brassil MM, Virgin HW, Nikolich-Zugich J, Moses AV, Gale M, Jr, Fruh K, Diamond MS. 2013. IRF-3, IRF-5, and IRF-7 coordinately regulate the type I IFN response in myeloid dendritic cells downstream of MAVS signaling. PLoS Pathog 9:e1003118. https://doi.org/10.1371/journal.ppat.1003118.
68. Daffis S, Samuel MA, Suthar MS, Keller BC, Gale M, Jr, Diamond MS. 2008. Interferon regulatory factor IRF-7 induces the antiviral alpha interferon response and protects against lethal West Nile virus infection. J Virol 82:8465–8475. https://doi.org/10.1128/JVI.00918-08.
69. Martina BE, Koraka P, van den Doel P, Rimmelzwaan GF, Haagmans BL, Osterhaus AD. 2008. DC-SIGN enhances infection of cells with glycosylated West Nile virus in vitro and virus replication in human dendritic cells induces production of IFN-α and TNF-α. Virus Res 135:64–71. https://doi.org/10.1016/j.virusres.2008.02.008.
70. Suthar MS, Ma DY, Thomas S, Lund JM, Zhang N, Daffis S, Rudensky AY, Bevan MJ, Clark EA, Kaja MK, Diamond MS, Gale M, Jr. 2010. IPS-1 is essential for the control of West Nile virus infection and immunity. PLoS Pathog 6:e1000757. https://doi.org/10.1371/journal.ppat.1000757.
71. Daffis S, Samuel MA, Suthar MS, Gale M, Jr, Diamond MS. 2008. Toll-like receptor 3 has a protective role against West Nile virus infection. J Virol 82:10349–10358. https://doi.org/10.1128/JVI.00935-08.
72. Daffis S, Suthar MS, Szretter KJ, Gale M, Jr, Diamond MS. 2009. Induction of IFN-β and the innate antiviral response in myeloid cells occurs through an IPS-1-dependent signal that does not require IRF-3 and IRF-7. PLoS Pathog 5:e1000607. https://doi.org/10.1371/journal.ppat.1000607.
73. Ben-Nathan D, Huitinga I, Lustig S, van Rooijen N, Kobiler D. 1996. West Nile virus neuroinvasion and encephalitis induced by macrophage depletion in mice. Arch Virol 141:459–469. https://doi.org/10.1007/BF01718310.
74. Purtha WE, Chachu KA, Virgin HW, IV, Diamond MS. 2008. Early B-cell activation after West Nile virus infection requires alpha/beta interferon but not antigen receptor signaling. J Virol 82:10964–10974. https://doi.org/10.1128/JVI.01646-08.
75. Martin AP, Marinkovic T, Canasto-Chibuque C, Latif R, Unkeless JC, Davies TF, Takahama Y, Furtado GC, Lira SA. 2009. CCR7 deficiency in NOD mice leads to thyroiditis and primary hypothyroidism. J Immunol 183:3073–3080. https://doi.org/10.4049/jimmunol.0900275.
76. Biancotto A, Grivel JC, Iglehart SJ, Vanpouille C, Lisco A, Sieg SF, Debernardo R, Garate K, Rodriguez B, Margolis LB, Lederman MM. 2007. Abnormal activation and cytokine spectra in lymph nodes of people chronically infected with HIV-1. Blood 109:4272–4279. https://doi.org/10.1182/blood-2006-11-055764.